ParB spreading on DNA requires cytidine triphosphate *in vitro*

Adam S. B. Jalal[1], Ngat T. Tran[1], and Tung B. K. Le[1*]

[1]Department of Molecular Microbiology

John Innes Centre, Norwich, NR4 7UH, United Kingdom

[*]*Correspondence: tung.le@jic.ac.uk*

ABSTRACT

In all living organisms, it is essential to transmit genetic information faithfully to the next generation. The SMC-ParAB-*parS* system is widely employed for chromosome segregation in bacteria. A DNA-binding protein ParB nucleates on *parS* sites and must associate with neighboring DNA, a process known as spreading, to enable efficient chromosome segregation. Despite its importance, how the initial few ParB molecules nucleating at *parS* sites recruit hundreds of further ParB to spread is not fully understood. Here, we reconstitute a *parS*-dependent ParB spreading event using purified proteins from *Caulobacter crescentus* and show that CTP is required for spreading. We further show that accumulation of ParB requires a closed DNA substrate and that a DNA-binding transcriptional regulator can act as a roadblock to attenuate spreading unidirectionally *in vitro*. Our biochemical reconstitutions recapitulate many observed *in vivo* properties of ParB and opens up avenues to investigate the interactions between ParB-*parS* with ParA and SMC.

INTRODUCTION

Faithful chromosome segregation is essential in all domains of life if daughter cells are each to inherit the full set of genetic information. The SMC-ParAB-*parS* complex is widely employed for chromosome segregation in bacteria[1–14]. The centromere *parS* is the first DNA locus to be segregated following chromosome replication[1,3,15,16]. ParB specifically nucleates on *parS* before spreading outwards to the flanking DNA and bridge/cage DNA together to form a large nucleoprotein network *in vivo*[17–24]. This nucleoprotein complex recruits SMC to disentangle and organize replicated DNA[11–14,25], ParB-*parS* also interacts with an ATPase ParA to power the segregation of replicated chromosomes[26–30]. Engineered strains harboring a nucleation-competent but spreading-defective mutant of *parB* are either unviable[4] or have elevated number of anucleate cells[3,7,9,16,31–34]. Despite the importance of spreading for proper chromosome segregation, the mechanism by which a few *parS*-bound ParB can recruit hundreds more ParB molecules to the vicinity of *parS* to assemble a high molecular-weight nucleoprotein complex is not fully understood.

Since the first report in 1995[35], ParB spreading has been observed *in vivo* by chromatin immunoprecipitation in multiple bacterial species[10,16–18,20,36]. The site-specific binding of ParB on *parS* has also been demonstrated[4,9,17,18,21,37–39], however a *parS*-dependent ParB spreading has resisted biochemical reconstitution[18–20,40,41]. Unsuccessful attempts to reconstitute *parS*-dependent spreading *in vitro* suggests that one or more additional factors might be missing. While reproducing a key result from Easter and Gober (2002)[42], we found that nucleoside triphosphate (NTP) could modulate the nucleation of ParB on *parS*. Personal communication with Stephan Gruber and the recent work by Osorio-Valeriano *et al* (2019)[43] and Soh *et al* (2019)[44] encouraged us to take steps further to investigate the role of NTP for ParB spreading in *Caulobacter crescentus*.

RESULTS AND DISCUSSION

Nucleoside triphosphate reduces the nucleation of *Caulobacter* ParB on *parS*.

Easter and Gober (2002) reported that ATP-bound *Caulobacter* ParA dissociated ParB from *parS*[42], however, the authors did not control for the effect of ATP alone on ParB-*parS* binding. To determine if ATP alone affects ParB-*parS* interaction, we attached a linear 20-bp biotinylated *parS* DNA to a streptavidin-coated probe to measure the bio-layer interference (BLI) (Figure 1). We monitored in real-time interactions between immobilized *parS* and purified *Caulobacter* ParB or a premixed ParB + ATP (Figure 1B). BLI assay monitors wavelength shifts (responses) resulting from changes in the optical thickness of the probe surface during association or dissociation of the analyte (see Materials and Methods). We observed less ParB associating with *parS* at steady state when ATP was included (Figure 1B). NTPs are highly negatively charged and could have affected protein-DNA interactions by binding non-specifically to the often positively charged DNA-binding domain. However, we found that ATP had no effect on another helix-turn-helix protein-DNA pair, for example, the well-characterized TetR-*tetO* interaction[45], thereby ruling our this possibility (Figure 1C). We further tested the effect of other NTPs on ParB binding to *parS* to find that GTP, CTP, and UTP also reduced the binding of ParB to *parS* at steady state (Figure 1B). Notably, CTP had the strongest effect on ParB-*parS* interaction (Figure 1B); an increasing concentration of CTP (but not CMP and less so for CDP) gradually reduced the binding of ParB to *parS* (Figure 1-figure supplement 1A and Figure 1D). In contrast, neither CTP nor other NTPs affected the TetR-*tetO* binding (Figure 1C). On closer inspection, we noted that ParB + CTP slowly dissociated from *parS* even before the probe was returned to a protein-free buffer (a gradual downward slope between 30th and 150th sec, Figure 1B), implying that CTP facilitated ParB removal from a 20-bp *parS* DNA. To investigate further, we monitored the dissociation rates of pre-bound NTP-free ParB-*parS* complexes after probes were returned to a protein-free buffer with or without CTP, we found ParB dissociating ~seven times faster in buffer with CTP than in buffer only solution (Figure 1E). Given the short length of a 20-bp *parS* DNA duplex that has only sufficient room for nucleation, our results suggest that CTP and other NTPs might decrease ParB nucleation on *parS*.

Cytidine triphosphate (CTP) facilitates ParB association with a closed DNA beyond nucleation

Next, we investigated the effect of NTPs on ParB spreading by employing a longer 169-bp *parS*-containing DNA fragment that has been labeled at both 5' ends with biotin (Figure 2A). Immobilizing a dual biotin-labeled DNA on a streptavidin-coated BLI probe created a closed DNA substrate[46] where both ends are blocked (Figure 2-figure supplement 1A-C). We monitored the interactions between immobilized DNA and purified *Caulobacter* ParB in the presence or absence of NTP-Mg^{2+}. In the absence of NTP, we observed the usual nucleation event on *parS* with 1 µM ParB protein (Figure 2A). We noted that the BLI signal was not as high as with a 20-bp *parS* probe (Figure 2A) due to a less efficient immobilization of a longer DNA fragment on the BLI probe. Premixing ATP, GTP, or UTP with ParB did not change the sensorgrams markedly (Figure 2A). However, the addition of CTP significantly increased the response by ~12 fold (Figure 2A), suggesting that more ParB associated with the 169-bp *parS* probe at steady state than by nucleation at *parS* alone. We observed that DNA-bound ParB was not salt-resistant and dissociated easily to the solution when the BLI probe was returned to a low-salt protein-free buffer without CTP (Figure 2A, dissociation phase). However, the dissociation of preformed ParB-CTP from DNA was slowed down by ~five fold if the probe was returned to a protein-free buffer supplemented with CTP (Figure 1-figure supplement 1B). The effect on the BLI response was not seen if Mg^{2+} was omitted (Figure 1-figure supplement 1C), neither did we observe an equivalent increase in response when a 169-bp dual biotin-labeled DNA containing a scrambled *parS* was employed instead (Figure 2A). Furthermore, we observed that a nucleation-competent but spreading-defective *Caulobacter* ParB (R104A)[10] mutant did not respond to the addition of CTP to the same extent as ParB (WT) (Figure 2B). Our results suggest that CTP is required for the extensive *parS*-dependent ParB spreading *in vitro*. Lastly, we performed BLI experiments for eight additional chromosomal ParB proteins from a diverse set of bacterial species and consistently observed the specific effect of CTP on enhancing ParB association with DNA *in vitro* (Figure 2-figure supplement 2). It is most likely that the enhancing effect of CTP on ParB-DNA association is conserved among ParB orthologs.

To independently verify the BLI data, we performed an *in vitro* pull-down of purified His-tagged *Caulobacter* ParB (Figure 2C). Streptavidin-coated paramagnetic beads were incubated with 2.8-kb dual biotin-labeled DNA fragments containing either *parS* or scrambled *parS* sites. Again, a dual biotin-labeled DNA formed a closed substrate on the surface of the beads. DNA-coated beads were incubated with purified *Caulobacter* ParB either in the presence or absence of NTP before being pulled down magnetically. Pulled-down ParB was released from beads and their protein level was analyzed by an α-His_6 immunoblot (Figure 2C). We found ~13-15 folds more pulled-down ParB when CTP was included (Figure 2C). No enrichment was observed when scrambled *parS*-coated beads were used, confirming that the extensive *in vitro* recruitment of ParB is dependent on *parS* (Figure 2C). Also, consistent with the BLI experiments, no further ParB recruitment was seen when ATP, GTP or UTP was included (Figure 2C). Furthermore, a nucleation-competent but spreading-defective ParB (R104A) variant was not enriched in our pull-down assay regardless of whether CTP was present or not (Figure 2C). Altogether, we suggest that a *parS*-dependent spreading of *Caulobacter* ParB on DNA requires CTP.

A closed DNA substrate is required for an increased ParB association with DNA

Next, we investigated whether an open-ended DNA substrate can also support ParB spreading *in vitro*. The 169-bp dual biotin-labeled DNA was designed with unique *Bam*HI and *Eco*RI recognition sites flanking the *parS* site (Figure 3A). To generate an opened DNA, we immerged the DNA-coated probes in buffers contained either *Bam*HI or *Eco*RI (Figure 3A-C and Figure 2-figure supplement 1D-E). Subsequently, probes were washed off restriction enzymes and returned to a binding buffer. Before restriction enzyme digestion, we again observed an enhanced ParB association with a closed DNA in the presence of CTP (Figure 3A). After restriction enzyme digestion, the inclusion of CTP had no effect on the BLI response, indicating that an opened DNA did not support the enrichment of ParB *in vitro* (Figure 3B-C). Consistent with BLI experiments, our pull-down assay also showed

that ParB failed to accumulate when a 2.8-kb dual biotin-labeled DNA was linearized by *Hind*III digestion (Figure 3D).

Next, we wondered if a tight protein-DNA binding could cap the open DNA end, thereby restoring ParB accumulation. To investigate this possibility, we constructed a 170-bp dual biotin-labeled DNA fragment that contains a single *parS* site, a *tetO* operator, and flanking restriction enzyme recognition sites for *Eco*RI and *Bam*HI (Figure 4A). With this closed DNA, we observed an enhanced ParB association with DNA in the presence of CTP (Figure 4A). Again, we generated an opened DNA via restriction enzyme digestion. Consistent with the previous experiment with a restricted 169-bp DNA probe, the addition of ParB + CTP had no effect on the BLI response (Figure 4B). However, it can be partially rescued by incubating a *Bam*HI-restricted DNA probe with a premix of ParB + CTP + TetR (Figure 4B). We reason that TetR binding at *tetO* capped the open DNA end, essentially generated a closed DNA. Our conclusion was further supported by results from an experiment in which a premixed ParB + CTP + TetR was tested against an *Eco*RI-restricted DNA instead (Figure 4C). Here, we did not observe an enhanced association of ParB with DNA even when TetR was included, most likely because of a persistent open DNA end that could not be blocked by TetR-*tetO* binding (Figure 4C). The ability of a DNA-bound TetR to block open DNA end and allows for an enhanced ParB association with DNA *in vitro* is consistent with previous ChIP-seq data that showed DNA-binding proteins or RNA polymerases could block or attenuate ParB spreading unidirectionally *in vivo*[17,18,21,36].

parS DNA increases the CTP binding and hydrolysis rate of *Caulobacter* ParB

Recently, Osorio-Valeriano *et al* (2019) and Soh *et al* (2019) reported that ParB from *Myxococcus xanthus* and *Bacillus subtilis* binds and hydrolyzes CTP[43,44]. Our *in vitro* results so far also hint at CTP binding directly to *Caulobacter* ParB to enhance ParB-DNA association in a *parS*-dependent manner. By employing a membrane-spotting assay (DRaCALA), we showed that *Caulobacter* ParB binds to radiolabeled CTP in the presence of *parS* DNA (Figure 5A). An excess of unlabeled CTP, but no other NTPs, could compete with radioactive CTP for binding to *Caulobacter* ParB (Figure 5B), suggesting that *Caulobacter* ParB does not bind or binds more weakly to other NTPs than to CTP. The CTP binding of ParB was reduced when a non-cognate DNA site (*NBS)*[47,48] was used instead of *parS* (Figure 5A). We also failed to detect CTP binding in our DRaCALA assay or by isothermal titration calorimetry (ITC) when DNA was omitted. Nevertheless, we robustly detected CTP hydrolysis to CDP and inorganic phosphate when *Caulobacter* ParB and CTP were included, albeit at a very low rate of ~ 0.4 CTP molecules per ParB per hour (Figure 5C). A background level of inorganic phosphate was observed when *Caulobacter* ParB was incubated with ATP, GTP, or UTP (Figure 5C). Crucially, the addition of a 22-bp *parS* DNA, but not a non-cognate 22-bp *NBS* DNA, increased CTP turnover rate seven fold to ~3 CTP molecules per ParB per hour (Figure 5C). Lastly, the CTP hydrolysis was reduced to the background level in the nucleation-competent but spreading-defective ParB (R104A) variant (Figure 5C). Altogether, our data suggest that *parS* DNA stimulates *Caulobacter* ParB to bind and hydrolyze CTP.

In this work, we report that a small molecule (CTP) is required to enable *Caulobacter* ParB proteins (as well as eight other chromosomal ParB proteins-Figure 2-figure supplement 2) to spread *in vitro*. Recently, Soh *et al* (2019) observed that F-plasmid and P1-plasmid ParB proteins also bind and hydrolyze CTP[44]. Hence, it is most likely that the effect of CTP on ParB spreading is universal among plasmid and chromosomal ParB orthologs. A classical mutant whose arginine-rich patch (G^{101}ERRxR) has been mutated to alanine e.g. ParB (R104A)[3,10] was not responsive to CTP, this observation suggests that CTP is bound to the N-terminal domain of *Caulobacter* ParB. Indeed, Soh *et al* (2019) reported a co-crystal structure that showed CDP binding to the arginine-rich patch at the N-terminal domain of *Bacillus* ParB (CTP has been hydrolyzed to CDP during crystallization)[44]. Osorio-Valeriano *et al* (2019) also showed a similar binding pocket of CTP at the N-terminal domain of *Myxococcus* ParB by hydrogen-deuterium exchange mass spectrometry (HDX-MS)[43]. Intriguingly, a co-crystal structure of a *Helicobacter pylori* ParB-*parS* complex, together with the *in vitro* magnetic-tweezer and single-molecule TIRF microscopy-based experiments with *Bacillus* and *Caulobacter* ParB showed that the N-terminal domain can oligomerize to bridge

DNA together without the need of an additional ligand[19,20,37,40,49]. It is possible that there are two different modes of actions of ParB on DNA: one for bridging DNA together (that does not require CTP) and another mode for a lateral spreading of ParB on DNA (that requires CTP).

The requirement of a closed DNA substrate for ParB spreading *in vitro* is suggestive of a lateral ParB diffusion along the DNA i.e. ParB can escape by running off a free DNA end (Figure 6). Inside cells, the spreading and bridging/caging of ParB have been inferred from the compact foci of fluorescently labeled ParB[9,16,21,50–54], presumably resulting from the concentration of fluorescent signal to a defined location in the cytoplasm. Nucleation-competent but spreading-defective ParB mutants formed no or very diffusive foci *in vivo*[20,55]. Recently, it has been observed that an artificially engineered double-strand break ~8 kb away from *parS* did not cause a dissolution of ParB foci in *Caulobacter* cells[56]. This result seemingly contradicted our findings that *Caulobacter* ParB spreading *in vitro* requires a closed DNA. However, we reason that the abundant DNA-bound transcription factors and RNA polymerases *in vivo* act as roadblocks to minimize ParB runoff (Figure 6). This barricading effect has been recapitulated in our experiments with TetR, a tight DNA-binding transcriptional regulator (Figure 4).

Our results so far suggest three distinct stages of ParB-DNA interactions:

Stage 1: ParB nucleates on *parS* (Figure 6A). Results from experiments in Figure 1 indicate that NTPs, especially CTP, modulate ParB nucleation on a *parS* site. Soh *et al* (2019) reported that CTP-bound ParB could form a closed protein ring even in the absence of *parS* DNA[44]. The DNA-binding domain (DBD) of a closed-ring ParB would be inaccessible to DNA, especially to a closed DNA substrate. It is likely that only apo-ParB and a transiently formed CDP-bound ParB (from CTP hydrolysis) are able to nucleate on *parS* (Figure 1 and Figure 6A). Supporting this interpretation, pre-mixing *Caulobacter* ParB with a non-hydrolyzable CTP analog (CTPγS) severely affected the nucleation step on *parS* (Figure 2-figure supplement 3A-B). Initially, we were surprised by a weak CTP binding and an extremely low CTP hydrolysis rate of *Caulobacter* and *Bacillus* ParB[44], however, this might be advantageous for the cells as a fraction of intracellular apo-ParB will be remained to nucleate on *parS*.

Stage 2: Nucleated ParB escapes from *parS* (Figure 6B-C). We showed that *Caulobacter* ParB-*parS* complex binds CTP, and this facilitates ParB dissociation from *parS* (Figure 1E). Soh *et al* (2019) reported that the DNA-binding domain of *Bacillus* ParB-CDP co-crystal structure is incompatible with *parS* binding[44] and this might enable ParB to escape from a high-affinity nucleation site to non-specific flanking DNA. Our observation of a low BLI response with an opened DNA (Figure 3 and Figure 4) implies that ParB proteins dissociate off the open DNA end well before the next ParB escapes from the *parS* nucleation site (Figure 6B-C). We suggest that the transition from a *parS*-bound ParB to a spreading ParB might be the rate-limiting step. Again, weak interaction between ParB and CTP might play a role in setting this rate-limiting step. For *Caulobacter* ParB, CTP hydrolysis by ParB-*parS* is not required for ParB to escape from the nucleation site. *Caulobacter* ParB could still spread on a 169-bp closed DNA when incubated with a non-hydrolyzable CTPγS (Figure 2-figure supplement 3A and C), even though both the association and dissociation phases were slowed down in comparison to when CTP was employed (Figure 2-figure supplement 3C).

Stage 3: ParB spreads or diffuses to non-specific DNA flanking *parS*. Our observation that *Caulobacter* ParB did not accumulate on an opened DNA suggests that *Caulobacter* ParB diffuses laterally along the DNA. Similarly, crosslinking experiments on *Bacillus* ParB[44] proposed that the ParB-CTP complex forms a sliding clamp that moves along the DNA[44]. From the observation in Figure 2-figure supplement 3C with CTPγS, we suggest that the diffusive *Caulobacter* ParB along the DNA is CTP bound. The extremely low CTP hydrolysis rate of *Caulobacter* ParB (~3 CTP molecules per ParB per hour) (Figure 5C) while ParB spreading could be observed by BLI within minutes (Figure 2A) also lends support to the interpretation that the diffusive spreading form of *Caulobacter* ParB is most likely CTP-bound (Figure 6). This is further backed up by the observation (Figure 1-figure supplement 1B) that DNA-bound ParB-CTP dissociated ~five times slower to a protein-free buffer containing CTP than to a buffer only solution i.e. CTP binding retains bound ParB on DNA more effectively.

FINAL PERSPECTIVES

In this work, we showed the enhancing effect of CTP on *Caulobacter* ParB spreading and further demonstrated that ParB spreading requires a closed DNA substrate with blocked ends and that a DNA-binding transcriptional regulator can act as a roadblock to attenuate spreading unidirectionally *in vitro*. Our real-time and label-free reconstitution of ParB spreading has successfully recapitulated many well-known aspects of ParB behaviors and is consistent with the recent works by Soh *et al* (2019)[44] and Osorio-Valeriano *et al* (2019)[43]. Beyond the biological significance of the findings, our label-free approaches to biochemical reconstitution obviate the often difficult and time-consuming task of site-specifically labeling proteins with fluorophores/chemical crosslinkers without affecting the function of proteins. Here, we have demonstrated the medium-throughput capability of our methodology by investigating the effect of CTP on the spreading of eight additional chromosomal ParB proteins. The ease and medium-throughput manner of our methodology will facilitate future works by the community to (i) investigate the effect of ParB spreading on the supercoiling state of the DNA, and (ii) contribute to an effort to reconstitute a ParB-dependent recruitment and loading of SMC, a feat so far has not been achieved *in vitro* for bacterial SMC complexes.

ACKNOWLEDGMENTS

This study was supported by the Royal Society University Research Fellowship (UF140053) and a BBSRC grant (BB/P018165/1) to T.B.K.L. A.S.B.J's PhD studentship was funded by the Royal Society (RG150448), and N.T.T was funded by the BBSRC grant-in-add (BBS/E/J/000C0683 to the John Innes Centre). We thank Dr. Wilma Ross (Department of Bacteriology, University of Wisconsin, Madison) for advice on DRaCALA assays, and Dr. Clare Stevenson (Biophysical Platform, John Innes Centre) for assistance in biophysical techniques. We thank Dr. César López Pastrana (Faculty of Physics, Technical University of Munich) for value feedback on the manuscript. We thank Dr. Stephan Gruber and Dr. Martin Thanbichler for sharing reagents and unpublished data.

AUTHOR CONTRIBUTION

Conceptualization: T.B.K.L. Investigation and data analysis: A.S.B.J, N.T.T, and T.B.K.L. Writing: T.B.K.L. Funding acquisition: T.B.K.L.

COMPETING INTERESTS

None

MATERIALS AND METHODS

Protein overexpression and purification

Full-length *Caulobacter* ParB (WT) and ParB (R104A) were purified as described previously[10,47,49]. Briefly, pET21b::ParB-$(His)_6$ (WT or R104A) was introduced into *E. coli* Rosetta pRARE competent cells (Novagen). A 10 mL overnight culture was used to inoculate 4 L of LB medium + carbenicillin + chloramphenicol. Cells were grown at 37˚C with shaking at 250 rpm to an OD_{600} of 0.4. The culture was then left to cool to 4˚C before isopropyl-β-D-thiogalactopyranoside (IPTG) was added to a final concentration of 1 mM. The culture was shaken for 3 hours at 30˚C before cells were harvested by centrifugation.

Pelleted cells were resuspended in a buffer containing 100 mM Tris-HCl pH 8.0, 300 mM NaCl, 10 mM Imidazole, 5% (v/v) glycerol, 1 µL of Benzonase nuclease (Sigma Aldrich), 1 mg of lysozyme (Sigma Aldrich), and an EDTA-free protease inhibitor tablet (Roche). The pelleted cells were then lyzed by sonication. The cell debris was removed via centrifugation at 28,000 g for 30 min and the supernatant was filtered through a 0.45 µm sterile filter (Sartorius Stedim). The protein was then loaded into a 1-ml HiTrap column (GE Healthcare) that had been equilibrated with buffer A [100 mM Tris-HCl pH 8.0, 300 mM NaCl, 10 mM Imidazole, and 5% glycerol]. Protein was eluted from the column using an increasing (10 mM to 500 mM) imidazole gradient in the same buffer. ParB-containing fractions were pooled and diluted to a conductivity of 16 mS/cm before being loaded onto a Heparin HP column (GE Healthcare) that had been equilibrated with 100 mM Tris-HCl pH 8.0, 25 mM NaCl, and 5% glycerol. Protein was eluted from the Heparin column using an increasing (25 mM to 1 M NaCl) salt gradient in the same buffer. ParB that was used for CTPase ENZCHECK assay and DRaCALA was further polished via a gel-filtration column. To do so, purified ParB was concentrated by centrifugation in an Amicon Ultra-15 3-kDa cut-off spin filters

(Merck) before being loaded into a Superdex 75 gel filtration column (GE Healthcare). The gel filtration column was pre-equilibrated with 100 mM Tris-HCl pH 8.0, 250 mM NaCl, and 1 mM $MgCl_2$.

C-terminally His-tagged TetR (class B, from Tn10) were expressed from *E. coli* Rosetta pRARE harboring a pET21b::TetR-His_6 plasmid (Table S1). TetR-His_6 were purified via a one-step Ni-affinity column using the exact buffers as employed for the purification of *Caulobacter* ParB-His_6.

N-terminally His-tagged MBP-tagged ParB (orthologous proteins from various bacterial species) were expressed from *E. coli* Rosetta pRARE harboring pET-His-MBP-TEV-DEST::ParB plasmids (Table S1). His_6-MBP-ParB were purified via a one-step Ni-affinity column as described previously[47].

Different batches of proteins were purified by A.S.B.J and N.T.T, and are consistent in all assays used in this work. Both biological (new sample preparations from a fresh stock aliquot) and technical (same sample preparation) replicates were performed for assays described in this study.

Construction of pET21b::TetR-His_6

DNA containing the coding sequence of TetR (class B, from Tn10) was chemically synthesized (gBlocks dsDNA fragments, IDT). This gBlocks fragment and a *Nde*I-*Hind*III-digested pET21b backbone were assembled together using a 2x Gibson master mix (NEB). 2.5 µL of each fragment at equimolar concentration was added to 5 µL 2x Gibson master mix (NEB), and the mixture was incubated at 50°C for 60 min. 5 µL was used to transform chemically-competent *E. coli* DH5α cells. Gibson assembly was possible due to a 23-bp sequence shared between the *Nde*I-*Hind*III-cut pET21b backbone and the gBlocks fragment. These 23-bp regions were incorporated during the synthesis of gBlocks fragments. The resulting plasmids were sequence verified by Sanger sequencing (Eurofins, Germany).

Construction of pENTR::ParB orthologs

The coding sequences of ParB orthologs were chemically synthesized (gBlocks dsDNA fragments, IDT) and cloned into pENTR-D-TOPO backbone (Invitrogen) by Gibson assembly (NEB). The resulting plasmids were sequence verified by Sanger sequencing (Eurofins, Germany).

Construction of pET-His-MBP-TEV-DEST::ParB orthologs

The *parB* genes were recombined into a Gateway-compatible destination vector pET-His-MBP-TEV-DEST[47] via an LR recombination reaction (Invitrogen). For LR recombination reactions: 1 µL of purified pENTR::*parB* was incubated with 1 µL of the destination vector pET-His-MBP-TEV-DEST, 1 µL of LR Clonase II master mix, and 2 µL of water in a total volume of 5 µL.

Construction of DNA substrates for BLI assays

All DNA constructs (Table S1) were designed in VectorNTI (Thermo Fisher) and were chemically synthesized (gBlocks dsDNA fragments, IDT). All linear DNA constructs were designed with an M13F and M13R homologous region at each end. To generate a dual biotin-labeled DNA substrate, PCR reactions were performed using a 2x GoTaq PCR master mix, biotin-labeled M13F and biotin-labeled M13R primers, and gBlocks fragments as template. PCR products were electrophoresed and gel purified.

Measurement of protein-DNA interaction by bio-layer interferometry (BLI)

Bio-layer interferometry experiments were conducted using a BLItz system equipped with Dip-and-Read Streptavidin (SA) Biosensors (ForteBio). BLItz monitors wavelength shifts (nm) resulting from changes in the optical thickness of the sensor surface during association or dissociation of the analyte. The streptavidin biosensor (ForteBio) was hydrated in a low-salt binding buffer [100 mM Tris-HCl pH 8.0, 100 mM NaCl, 1 mM $MgCl_2$, and 0.005% Tween 20] for at least 10 min before each experiment. Biotinylated dsDNA was immobilized onto the surface of the SA biosensor through a cycle of 30 s Baseline, 120 s Association, and 120 s Dissociation. Briefly, the tip of the biosensor was dipped into a binding buffer for 30 s to establish the baseline, then to 1 µM biotinylated dsDNA for 120 s, and finally to a low salt binding buffer for 120 s to allow for dissociation. For experiments where a closed DNA was cleaved to generate a free DNA end, DNA-coated tips were dipped into 300 µL of

cutting solution [270 µL of water, 30 µL of 10x CutSmart buffer (NEB), and 4 µL of *Eco*RI or *Bam*HI restriction enzyme] for 30 min at 37°C.

After the immobilization of DNA on the sensor, association reactions were monitored at 1 µM dimer concentration of ParB (with or without 1 µM TetR or NTPs at various concentrations) for 120s. At the end of each binding step, the sensor was transferred into a protein-free binding buffer to follow the dissociation kinetics for 120s. The sensor can be recycled by dipping in a high-salt buffer [100 mM Tris-HCl pH 8.0, 1000 mM NaCl, 1 mM $MgCl_2$, and 0.005% Tween 20] for 5 min to remove bound ParB. All sensorgrams recorded during BLI experiments were analyzed using the BLItz analysis software (BLItz Pro version 1.2, ForteBio) and replotted in R for presentation. Each experiment was triplicated, the standard deviation of triplicated sensorgrams is less than six percent, and a representative sensorgram was presented in each figure.

To verify that dual biotin-labeled DNA fragments formed a closed substrate on the surface of the BLI probe, we performed double digestion with Exonuclease T7 and Exonuclease VII (NEB) (Figure 2-figure supplement 1). DNA-coated tips were dipped into 300 µL of cutting solution [270 µL of water, 30 µL of 10x RE buffer 4 (NEB), 2 µL of exonuclease T7 and 2 µL of exonuclease VII] for 30 min at 25°C. Tips were then cut off from the plastic adaptor (Figure 2-figure supplement 1B) and immerged into a GoTaq PCR master-mix [25 µL water, 25 µL 2x GoTaq, 0.5 µL M13F oligo, and 0.5 µL M13R oligo]. Ten cycles of PCR were performed, and the PCR products were resolved on 2% agarose gels (Figure 2-figure supplement 1).

CTP (stock concentration: 100 mM) used in BLI assays was purchased from ThermoFisher. CTPγS (stock concentration: 90 mM) was a generous gift from Stephan Gruber and Young-Min Soh. Another non-hydrolyzable analog (CMP-PNP, Jena Biosciences) was unsuitable for our assays as *Caulobacter* ParB does not bind CMP-PNP as well as CTP (Figure 2-figure supplement 3A).

Construction of DNA substrates for pull-down assays

A 260-bp DNA fragment containing *Caulobacter parS* sites (genomic position: 4034789-4035048)[10] or scrambled *parS* sites were chemically synthesized (gBlocks fragments, IDT). These DNA fragments were subsequently 5' phosphorylated using T4 PNK enzyme (NEB), then cloned into a *Sma*I-cut pUC19 using T4 DNA ligase (NEB). The two resulting plasmids are pUC19::260bp-*parS* and pUC19::260bp-scrambled *parS* (Table S1). These plasmids were sequence verified by Sanger sequencing (Eurofins, Germany). To generate dual biotin-labeled DNA substrates, we performed PCR using a pair of biotinylated primers: around_pUC19_F and around_pUC19_R, and either pUC19::260bp-*parS* or pUC19::260bp-scrambled *parS* as a template. Phusion DNA polymerase (NEB) was employed for this round-the-horn PCR reaction. The resulting ~2.8-kb linear DNA fragments were gel-purified and eluted in 50 µL of distilled autoclaved water.

Pull-down assays

Paramagnetic MyOne Streptavidin C1 Dyna beads (Thermo Fisher) were used for pull-down assays. 30 µL of beads were washed twice in 500 µL of high-salt wash buffer [100 mM Tris-HCl pH 8.0, 1 M NaCl, 1 mM $MgCl_2$, and 0.005% Tween 20] and once in 100 µL binding buffer [100 mM Tris-HCl pH 8.0, 100 mM NaCl, 1 mM $MgCl_2$, and 0.005% Tween 20] by repeating a cycle of resuspension and pull-down by magnetic attraction. 5 µL of dual biotin-labeled DNA substrate was incubated with 30 µL of beads in 100 µL binding buffer for 30 min at room temperature. The reaction was occasionally mixed by pipetting up and down several times. Afterward, DNA-coated beads were washed once in 500 µL high-salt buffer [100 mM Tris-HCl pH 8.0, 1000 mM NaCl, 1 mM $MgCl_2$, and 0.005% Tween 20] and once in 500 µL of binding buffer. Finally, DNA-coated beads were resuspended in 300 µL of binding buffer. 96 µL of the resuspended beads were used for each pull-down assay. 4 µL of *Caulobacter* ParB-His_6 (WT or R104A mutant, stock concentration: 25 µM) were added to 96 µL of suspended beads. NTPs were either omitted or added to the suspended beads to the final concentration of 1 mM. The mixture was pipetted up and down several times and was left to incubate at room temperature for 5 min. Beads were then pulled down magnetically and unwanted supernatant discarded. DNA-coated beads (now with bound protein) were then

washed once with 500 µL of binding buffer and once with 100 µL of the same buffer. The unwanted supernatant was discarded, and the left-over beads were resuspended in 30 µL of 1x SDS-PAGE sample buffer. Each experiment was triplicated, and a representative immunoblot was presented.

Immunoblot analysis

For immunoblot analysis, magnetic beads were resuspended directly in 1x SDS sample buffer, then heated to 42°C for 15 min before loading to 12% Novex Tris-Glycine SDS-PAGE gels (Thermo Fisher). The eluted protein was electrophoresed at 150 V for 60 min. Resolved proteins were transferred to polyvinylidene fluoride membranes using the Trans-Blot Turbo Transfer System (BioRad) and probed with 1:5,000 dilution of α-His_6 HRP-conjugated antibody (Abcam). Blots were imaged and analyzed using an Amersham Imager 600 (GE Healthcare) and Image Studio Lite version 5.2 (LI-COR Biosciences). The band intensities were quantified for lanes 5 and 6 (Figure 2C and Figure 3D), and the range of fold difference between replicates was reported.

Differential radial capillary action of ligand assay (DRaCALA) or membrane-spotting assay

Purified *Caulobacter* ParB-His6 or TetR-His_6 (final concentration: 25 µM) were incubated with 3 nM radiolabeled P^{32}-α-CTP (Perkin Elmer), 30 µM of unlabeled cold CTP (Thermo Fisher), 0.5 µM of 22-bp *parS* or *NBS* DNA duplex in the reaction buffer [100 mM Tris pH 8.0, 100 mM NaCl, and 10 mM $MgCl_2$] for 5 minutes at room temperature. For the NTP competition assay, the mixture was further supplemented with 500 µM of either unlabeled cold CTP, ATP, GTP, or UPT. Four µL of samples were spotted slowly onto a dry nitrocellulose membrane and air-dried. The nitrocellulose membrane was wrapped in cling film before being exposed to a phosphor screen (GE Healthcare) for two minutes. Each DRaCALA assay was triplicated and a representative autoradiograph was shown.

DNA preparation for EnzCheck Phosphate assay and DRaCALA

A 22-bp palindromic single-stranded DNA fragment (*parS*: GGATGTTTCACGTGAAACA TCC or *NBS*: GGATATTTCCCGGGAAATATCC) [100 µM in 1 mM Tris-HCl pH 8.0, 5 mM NaCl buffer] was heated at 98°C for 5 min before being left to cool down to room temperature overnight to form 50 µM double-stranded *parS* or *NBS* DNA. The sequences of *parS* and *NBS* are underlined.

Measurement of NTPase activity by EnzCheck Phosphate assay

NTP hydrolysis was monitored using an EnzCheck Phosphate Assay Kit (Thermo Fisher). 100 µL samples containing a reaction buffer supplemented with 1 mM of NTP and 1 µM ParB (WT or R104A) were assayed in a Biotek EON plate reader at 25°C for 15 hours with readings every minute. 1 mL of the reaction buffer typically contained: 740 µL Ultrapure water, 50 µL 20x customized reaction buffer [100 mM Tris pH 8.0, 2 M NaCl, and 20 mM $MgCl_2$], 200 µL MESG substrate solution, and 10 µL purine nucleoside phosphorylase (1 U). Reactions with buffer only, buffer + protein only or buffer + NTP only were also included as controls. The plates were shaken at 280 rpm continuously for 15 hours at 25°C. The inorganic phosphate standard curve was also constructed according to the manual. Each assay was triplicated. The results were analyzed using R and the NTPase rates were calculated using a linear regression fitting in R.

REFERENCES

1. Livny, J., Yamaichi, Y. & Waldor, M. K. Distribution of Centromere-Like parS Sites in Bacteria: Insights from Comparative Genomics. *J. Bacteriol.* **189**, 8693–8703 (2007).

2. Ireton, K., Gunther, N. W. & Grossman, A. D. spo0J is required for normal chromosome segregation as well as the initiation of sporulation in Bacillus subtilis. *J. Bacteriol.* **176**, 5320–5329 (1994).

3. Lin, D. C.-H. & Grossman, A. D. Identification and Characterization of a Bacterial Chromosome Partitioning Site. *Cell* **92**, 675–685 (1998).

4. Mohl, D. A., Easter, J. & Gober, J. W. The chromosome partitioning protein, ParB, is required for cytokinesis in Caulobacter crescentus. *Mol. Microbiol.* **42**, 741–755 (2001).

5. Fogel, M. A. & Waldor, M. K. A dynamic, mitotic-like mechanism for bacterial chromosome segregation. *Genes Dev.* **20**, 3269–3282 (2006).

6. Donczew, M. *et al.* ParA and ParB coordinate chromosome segregation with cell elongation and division during Streptomyces sporulation. *Open Biology* **6**, 150263 (2016).

7. Kawalek, A., Bartosik, A. A., Glabski, K. & Jagura-Burdzy, G. Pseudomonas aeruginosa partitioning protein ParB acts as a nucleoid-associated protein binding to multiple copies of a parS-related motif. *Nucleic Acids Res.* **46**, 4592–4606 (2018).

8. Jakimowicz, D., Chater, K. & Zakrzewska-Czerwi´nska, J. The ParB protein of Streptomyces coelicolor A3(2) recognizes a cluster of parS sequences within the origin-proximal region of the linear chromosome. *Molecular Microbiology* **45**, 1365–1377 (2002).

9. Harms, A., Treuner-Lange, A., Schumacher, D. & Sogaard-Andersen, L. Tracking of chromosome and replisome dynamics in Myxococcus xanthus reveals a novel chromosome arrangement. *PLoS Genet* **9**, e1003802 (2013).

10. Tran, N. T. *et al.* Permissive zones for the centromere-binding protein ParB on the Caulobacter crescentus chromosome. *Nucleic Acids Res* **46**, 1196–1209 (2018).

11. Tran, N. T., Laub, M. T. & Le, T. B. K. SMC Progressively Aligns Chromosomal Arms in Caulobacter crescentus but Is Antagonized by Convergent Transcription. *Cell Rep* **20**, 2057–2071 (2017).

12. Gruber, S. & Errington, J. Recruitment of condensin to replication origin regions by ParB/SpoOJ promotes chromosome segregation in B. subtilis. *Cell* **137**, 685–96 (2009).

13. Sullivan, N. L., Marquis, K. A. & Rudner, D. Z. Recruitment of SMC by ParB-parS organizes the origin region and promotes efficient chromosome segregation. *Cell* **137**, 697–707 (2009).

14. Wang, X., Brandão, H. B., Le, T. B. K., Laub, M. T. & Rudner, D. Z. Bacillus subtilis SMC complexes juxtapose chromosome arms as they travel from origin to terminus. *Science* **355**, 524–527 (2017).

15. Toro, E., Hong, S.-H., McAdams, H. H. & Shapiro, L. Caulobacter requires a dedicated mechanism to initiate chromosome segregation. *PNAS* **105**, 15435–15440 (2008).

16. Lagage, V., Boccard, F. & Vallet-Gely, I. Regional Control of Chromosome Segregation in Pseudomonas aeruginosa. *PLOS Genetics* **12**, e1006428 (2016).

17. Breier, A. M. & Grossman, A. D. Whole-genome analysis of the chromosome partitioning and sporulation protein Spo0J (ParB) reveals spreading and origin-distal sites on the Bacillus subtilis chromosome. *Molecular Microbiology* **64**, 703–718 (2007).

18. Murray, H., Ferreira, H. & Errington, J. The bacterial chromosome segregation protein Spo0J spreads along DNA from parS nucleation sites. *Molecular Microbiology* **61**, 1352–1361 (2006).

19. Taylor, J. A. *et al.* Specific and non-specific interactions of ParB with DNA: implications for chromosome segregation. *Nucleic Acids Res* **43**, 719–731 (2015).

20. Graham, T. G. W. *et al.* ParB spreading requires DNA bridging. *Genes Dev.* **28**, 1228–1238 (2014).

21. Sanchez, A. *et al.* Stochastic Self-Assembly of ParB Proteins Builds the Bacterial DNA Segregation Apparatus. *Cell Syst.* **1**, 163–173 (2015).

22. Debaugny, R. E. *et al.* A conserved mechanism drives partition complex assembly on bacterial chromosomes and plasmids. *Mol. Syst. Biol.* **14**, e8516 (2018).

23. Broedersz, C. P. *et al.* Condensation and localization of the partitioning protein ParB on the bacterial chromosome. *PNAS* **111**, 8809–8814 (2014).

24. Funnell, B. E. ParB Partition Proteins: Complex Formation and Spreading at Bacterial and Plasmid Centromeres. *Front Mol Biosci* **3**, 44 (2016).

25. Minnen, A., Attaiech, L., Thon, M., Gruber, S. & Veening, J.-W. SMC is recruited to oriC by ParB and promotes chromosome segregation in Streptococcus pneumoniae. *Mol. Microbiol.* **81**, 676–688 (2011).

26. Lim, H. C. *et al.* Evidence for a DNA-relay mechanism in ParABS-mediated chromosome segregation. *Elife* **3**, e02758 (2014).

27. Vecchiarelli, A. G., Neuman, K. C. & Mizuuchi, K. A propagating ATPase gradient drives transport of surface-confined cellular cargo. *Proc. Natl. Acad. Sci. U.S.A.* **111**, 4880–4885 (2014).

28. Vecchiarelli, A. G., Mizuuchi, K. & Funnell, B. E. Surfing biological surfaces: exploiting the nucleoid for partition and transport in bacteria. *Molecular Microbiology* **86**, 513–523 (2012).

29. Hwang, L. C. *et al.* ParA-mediated plasmid partition driven by protein pattern self-organization. *The EMBO Journal* **32**, 1238–1249 (2013).

30. Leonard, T. A., Butler, P. J. & Löwe, J. Bacterial chromosome segregation: structure and DNA binding of the Soj dimer--a conserved biological switch. *EMBO J.* **24**, 270–282 (2005).

31. Jecz, P., Bartosik, A. A., Glabski, K. & Jagura-Burdzy, G. A single parS sequence from the cluster of four sites closest to oriC is necessary and sufficient for proper chromosome segregation in Pseudomonas aeruginosa. *PLoS ONE* **10**, e0120867 (2015).

32. Attaiech, L., Minnen, A., Kjos, M., Gruber, S. & Veening, J.-W. The ParB-parS Chromosome Segregation System Modulates Competence Development in Streptococcus pneumoniae. *mBio* **6**, e00662-15 (2015).

33. Yu, W., Herbert, S., Graumann, P. L. & Götz, F. Contribution of SMC (Structural Maintenance of Chromosomes) and SpoIIIE to Chromosome Segregation in Staphylococci. *J Bacteriol* **192**, 4067–4073 (2010).

34. Lee, P. S. & Grossman, A. D. The chromosome partitioning proteins Soj (ParA) and Spo0J (ParB) contribute to accurate chromosome partitioning, separation of replicated sister origins, and regulation of replication initiation in Bacillus subtilis. *Mol. Microbiol.* **60**, 853–869 (2006).

35. Lynch, A. S. & Wang, J. C. SopB protein-mediated silencing of genes linked to the sopC locus of Escherichia coli F plasmid. *PNAS* **92**, 1896–1900 (1995).

36. Rodionov, O., Lobocka, M. & Yarmolinsky, M. Silencing of genes flanking the P1 plasmid centromere. *Science* **283**, 546–549 (1999).

37. Chen, B.-W., Lin, M.-H., Chu, C.-H., Hsu, C.-E. & Sun, Y.-J. Insights into ParB spreading from the complex structure of Spo0J and parS. *Proc. Natl. Acad. Sci. U.S.A.* **112**, 6613–6618 (2015).

38. Surtees, J. A. & Funnell, B. E. The DNA Binding Domains of P1 ParB and the Architecture of the P1 Plasmid Partition Complex. *J. Biol. Chem.* **276**, 12385–12394 (2001).

39. Ah-Seng, Y., Rech, J., Lane, D. & Bouet, J.-Y. Defining the role of ATP hydrolysis in mitotic segregation of bacterial plasmids. *PLoS Genet.* **9**, e1003956 (2013).

40. Fisher, G. L. *et al.* The structural basis for dynamic DNA binding and bridging interactions which condense the bacterial centromere. *Elife* **6**, (2017).

41. Madariaga-Marcos, J., Pastrana, C. L., Fisher, G. L., Dillingham, M. S. & Moreno-Herrero, F. ParB dynamics and the critical role of the CTD in DNA condensation unveiled by combined force-fluorescence measurements. *Elife* **8**, (2019).

42. Easter, J. & Gober, J. W. ParB-Stimulated Nucleotide Exchange Regulates a Switch in Functionally Distinct ParA Activities. *Molecular Cell* **10**, 427–434 (2002).

43. Manuel Osorio-Valeriano *et al.* ParB-type DNA segregation proteins are CTP-dependent molecular switches. *Cell* (in press).

44. Soh, Y.-M. *et al.* Self-organization of parS centromeres by the ParB CTP hydrolase. *Science* (2019) doi:10.1126/science.aay3965.

45. Saenger, W., Orth, P., Kisker, C., Hillen, W. & Hinrichs, W. The Tetracycline Repressor—A Paradigm for a Biological Switch. *Angewandte Chemie International Edition* **39**, 2042–2052 (2000).

46. Onn, I. & Koshland, D. In vitro assembly of physiological cohesin/DNA complexes. *PNAS* **108**, 12198–12205 (2011).

47. Jalal, A. S. B. *et al.* Evolving a new protein-DNA interface via sequential introduction of permissive and specificity-switching mutations. *bioRxiv* 724823 (2019) doi:10.1101/724823.

48. Wu, L. J. & Errington, J. Coordination of cell division and chromosome segregation by a nucleoid occlusion protein in Bacillus subtilis. *Cell* **117**, 915–925 (2004).

49. Jalal, A. S. B. *et al.* Structural and biochemical analyses of Caulobacter crescentus ParB reveal the role of its N-terminal domain in chromosome segregation. *bioRxiv* 816959 (2019) doi:10.1101/816959.

50. Thanbichler, M. & Shapiro, L. MipZ, a Spatial Regulator Coordinating Chromosome Segregation with Cell Division in Caulobacter. *Cell* **126**, 147–162 (2006).

51. Kusiak, M., Gapczyńska, A., Płochocka, D., Thomas, C. M. & Jagura-Burdzy, G. Binding and Spreading of ParB on DNA Determine Its Biological Function in Pseudomonas aeruginosa. *J. Bacteriol.* **193**, 3342–3355 (2011).

52. Lin, D. C., Levin, P. A. & Grossman, A. D. Bipolar localization of a chromosome partition protein in Bacillus subtilis. *Proc. Natl. Acad. Sci. U.S.A.* **94**, 4721–4726 (1997).

53. Glaser, P. *et al.* Dynamic, mitotic-like behavior of a bacterial protein required for accurate chromosome partitioning. *Genes Dev.* **11**, 1160–1168 (1997).

54. Erdmann, N., Petroff, T. & Funnell, B. E. Intracellular localization of P1 ParB protein depends on ParA and parS. *Proc Natl Acad Sci U S A* **96**, 14905–14910 (1999).

55. Song, D., Rodrigues, K., Graham, T. G. W. & Loparo, J. J. A network of cis and trans interactions is required for ParB spreading. *Nucleic Acids Res.* **45**, 7106–7117 (2017).

56. Badrinarayanan, A., Le, T. B. K. & Laub, M. T. Rapid pairing and resegregation of distant homologous loci enables double-strand break repair in bacteria. *J Cell Biol* **210**, 385–400 (2015).

FIG. 1

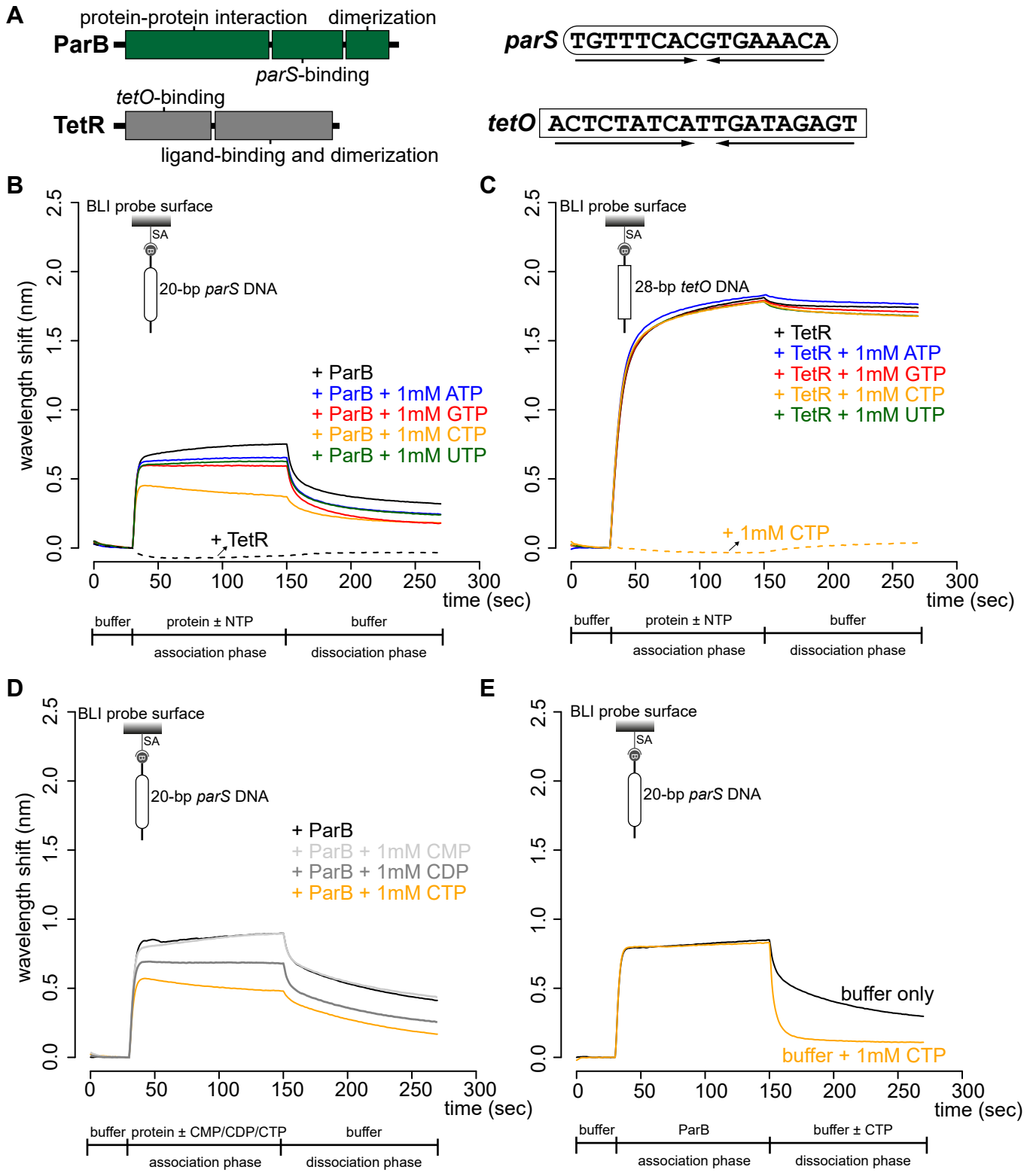

Figure 1. Nucleoside triphosphate reduces the nucleation of *Caulobacter* ParB at *parS*. (A) The domain architecture of ParB (dark green) and TetR (grey), and their respective DNA-binding sites *parS* and *tetO*. Convergent arrows below DNA-binding sites indicate that *parS* and *tetO* are palindromic. **(B)** Bio-layer interferometric (BLI) analysis of the interaction between a premix of 1 μM ParB dimer ± 1 mM NTP and a 20-bp DNA duplex containing *parS*. Biotinylated DNA fragments were immobilized onto the surface of a Streptavidin (SA)-coated probe (See Materials and Methods). The BLI probe was dipped into a buffer only solution (0-30 sec), then to a premix of protein ± NTP (30-150 sec: association phase), and finally returned to a buffer only solution (150-270 sec: dissociation phase). Sensorgrams were recorded over time. **(C)** BLI analysis of the interaction between a premix of 1 μM TetR-His_6 ± 1 mM NTP and a 28-bp DNA duplex containing *tetO*. **(D)** BLI analysis of the interaction between a premix of 1 μM *Caulobacter* ParB-His_6 ± 1 mM cytidine mono-, di- , or triphosphate, and a 20-bp *parS* DNA. **(E)** BLI analysis of the interaction between 1 μM *Caulobacter* ParB-His_6 (without CTP) and a 20-bp *parS* DNA. For the dissociation phase, the probe was returned to a buffer only or buffer supplemented with 1 mM CTP solution. Each BLI experiment was triplicated and a representative sensorgram was presented.

FIG. 2

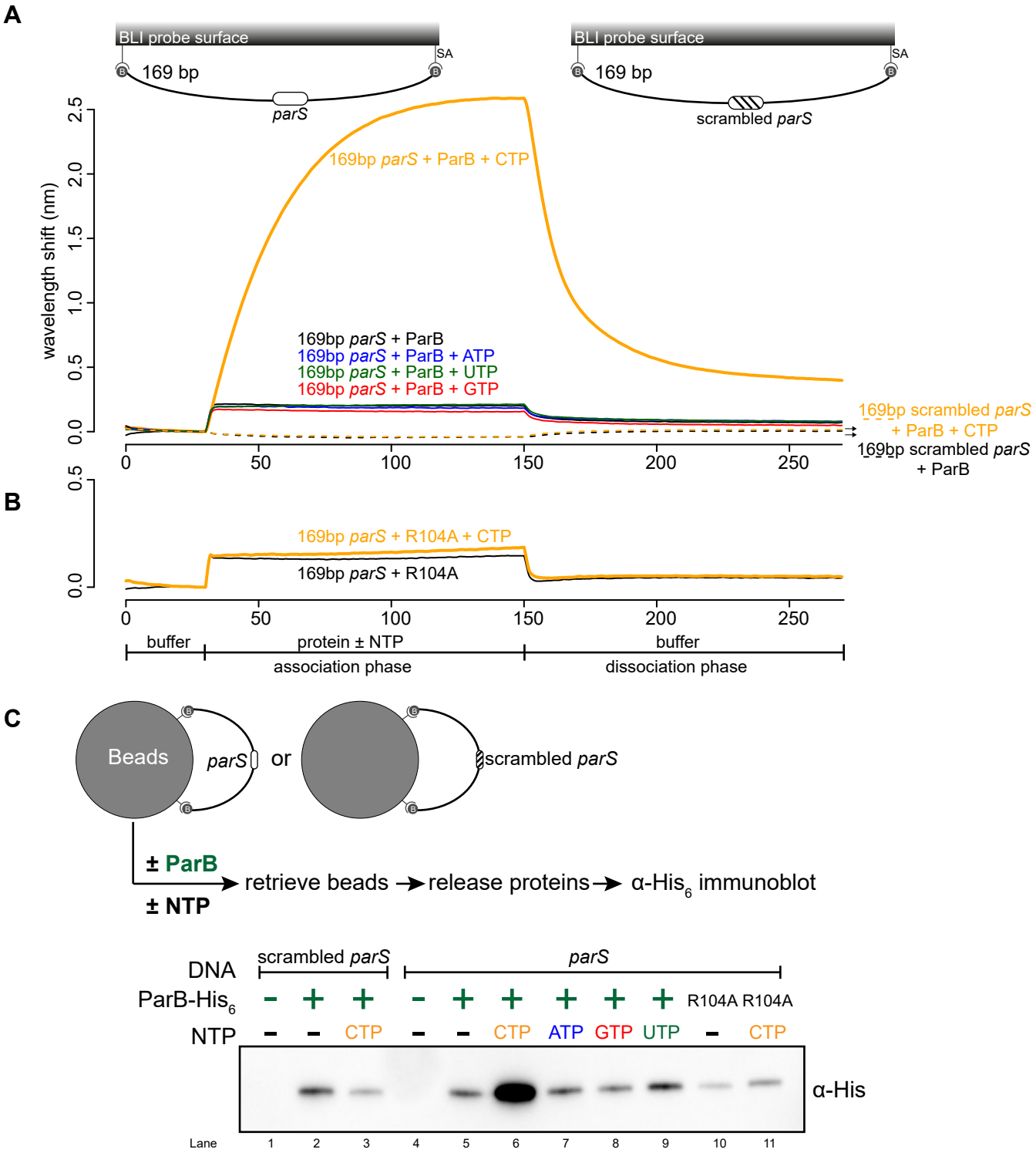

Figure 2. Cytidine triphosphate (CTP) facilitates ParB association with a closed DNA beyond nucleation. (A) BLI analysis of the interaction between a premix of 1 μM *Caulobacter* ParB-His$_6$ ± 1 mM NTP and a 169-bp dual biotin-labeled DNA containing a *parS* or a scrambled *parS* site. Interactions between a dual biotinylated DNA and streptavidin (SA)-coated probe created a closed DNA substrate where both ends are blocked (see the schematic of the BLI probe above the sensorgram). **(B)** Interactions between a nucleation-competent but spreading-defective ParB (R104) variant with a 169-bp *parS* DNA fragment in the presence or absence of CTP were also recorded. Each BLI experiment was triplicated and a representative sensorgram was presented. **(C)** Schematic of the pull-down assay and immunoblot analysis of pulled-down *Caulobacter* ParB-His$_6$. The length of bound DNA is ~2.8 kb. Beads were incubated with ParB protein for five minutes before being pulled down magnetically.

FIG. 3

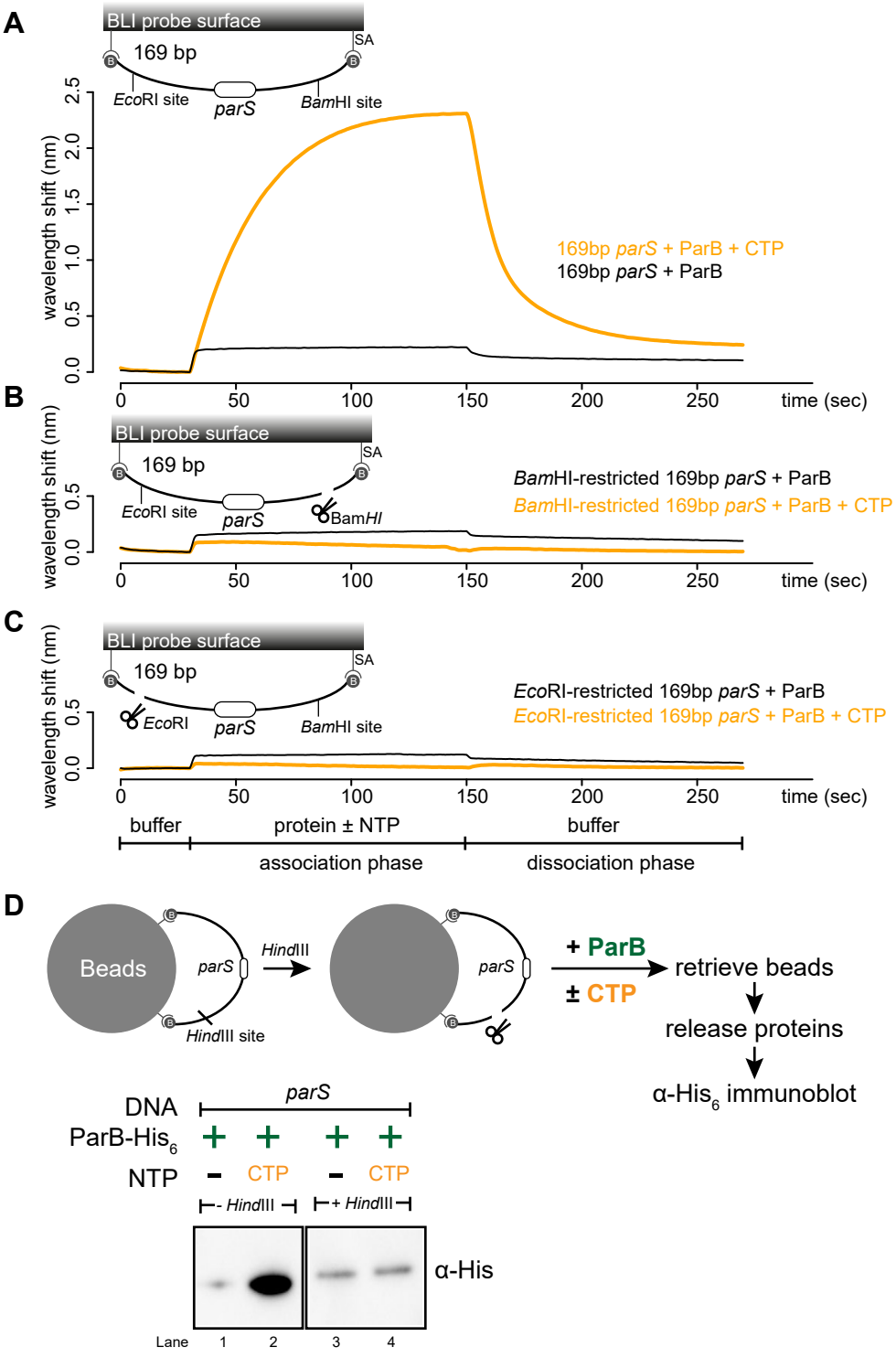

Figure 3. A closed DNA substrate is required for an increased association of ParB with DNA. **(A)** BLI analysis of the interaction between a premix of 1 μM *Caulobacter* ParB-His$_6$ ± 1mM CTP and a 169-bp dual biotin-labeled *parS* DNA. The schematic of the DNA fragment with the relative positions of *parS* and restriction enzyme recognition sites are shown above the sensorgram. **(B)** Same as panel A but immobilized DNA fragments have been restricted with *Bam*HI before BLI analysis. **(C)** Same as panel A but immobilized DNA fragments have been restricted with *Eco*RI before BLI analysis. Each BLI experiment was triplicated and a representative sensorgram was presented. **(D)** Schematic of the pull-down assay and immunoblot analysis of pulled-down *Caulobacter* ParB-His$_6$. Lanes 1 to 4 were from the same blot and were spliced together for presentation purpose. The length of bound DNA is ~2.8 kb. Beads were incubated with ParB protein for five minutes before being pulled down magnetically.

FIG. 4

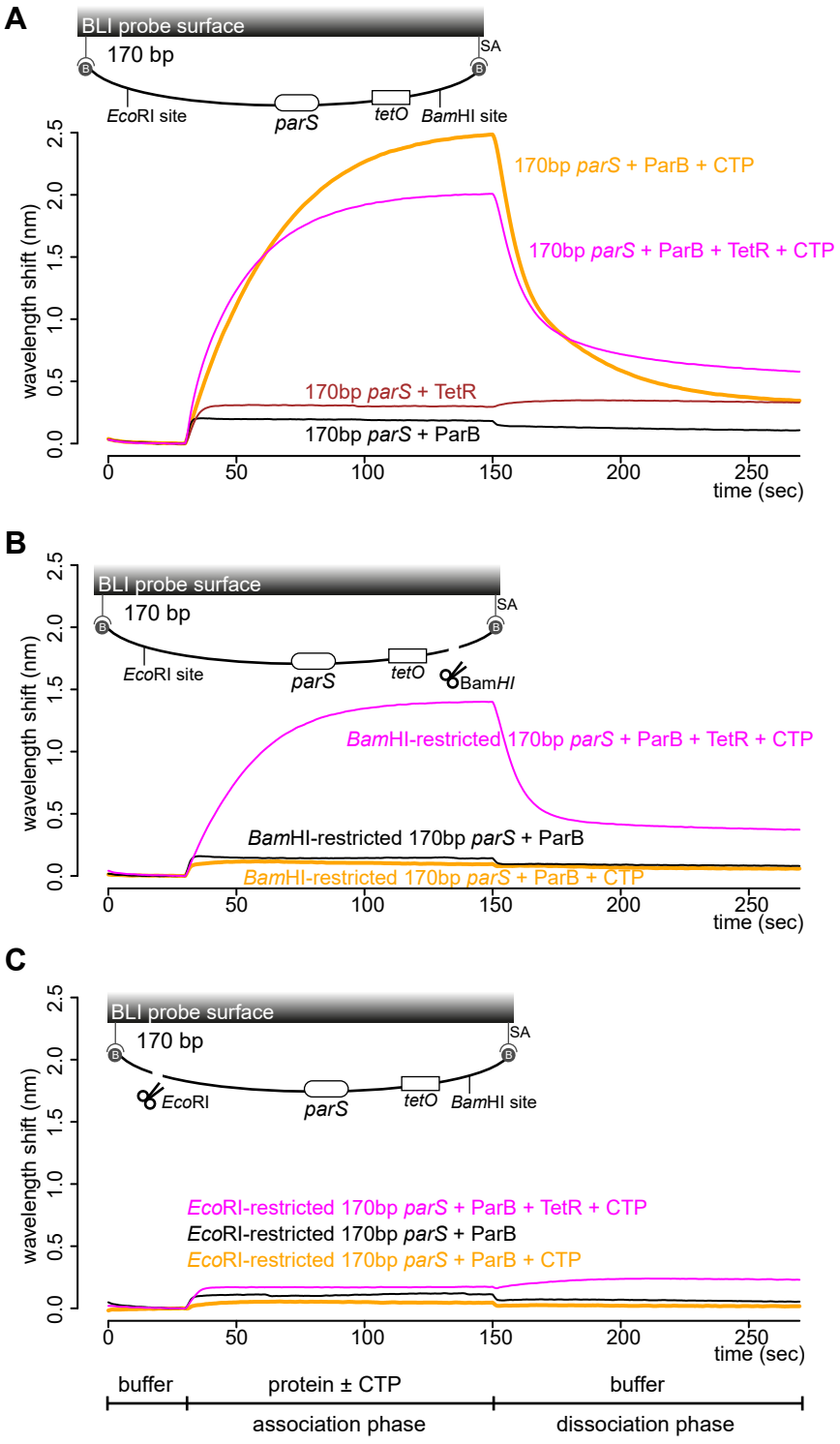

Figure 4. TetR-*tetO* binding restores ParB association with an opened DNA substrate. (A) BLI analysis of the interaction between a premix of 1 μM *Caulobacter* ParB-His$_6$ ± 1mM CTP ± 1 μM TetR-His$_6$ and a 170-bp dual biotin-labeled DNA containing a *parS* site. The schematic of the DNA fragment together with the relative positions of *parS*, *tetO*, and restriction enzyme recognition sites are shown above the sensorgram. **(B)** Same as panel A but immobilized DNA fragments have been restricted with *Bam*HI before BLI analysis. **(C)** Same as panel A but immobilized DNA fragments have been restricted with *Eco*RI before BLI analysis. Each BLI experiment was triplicated and a representative sensorgram was presented.

FIG. 5

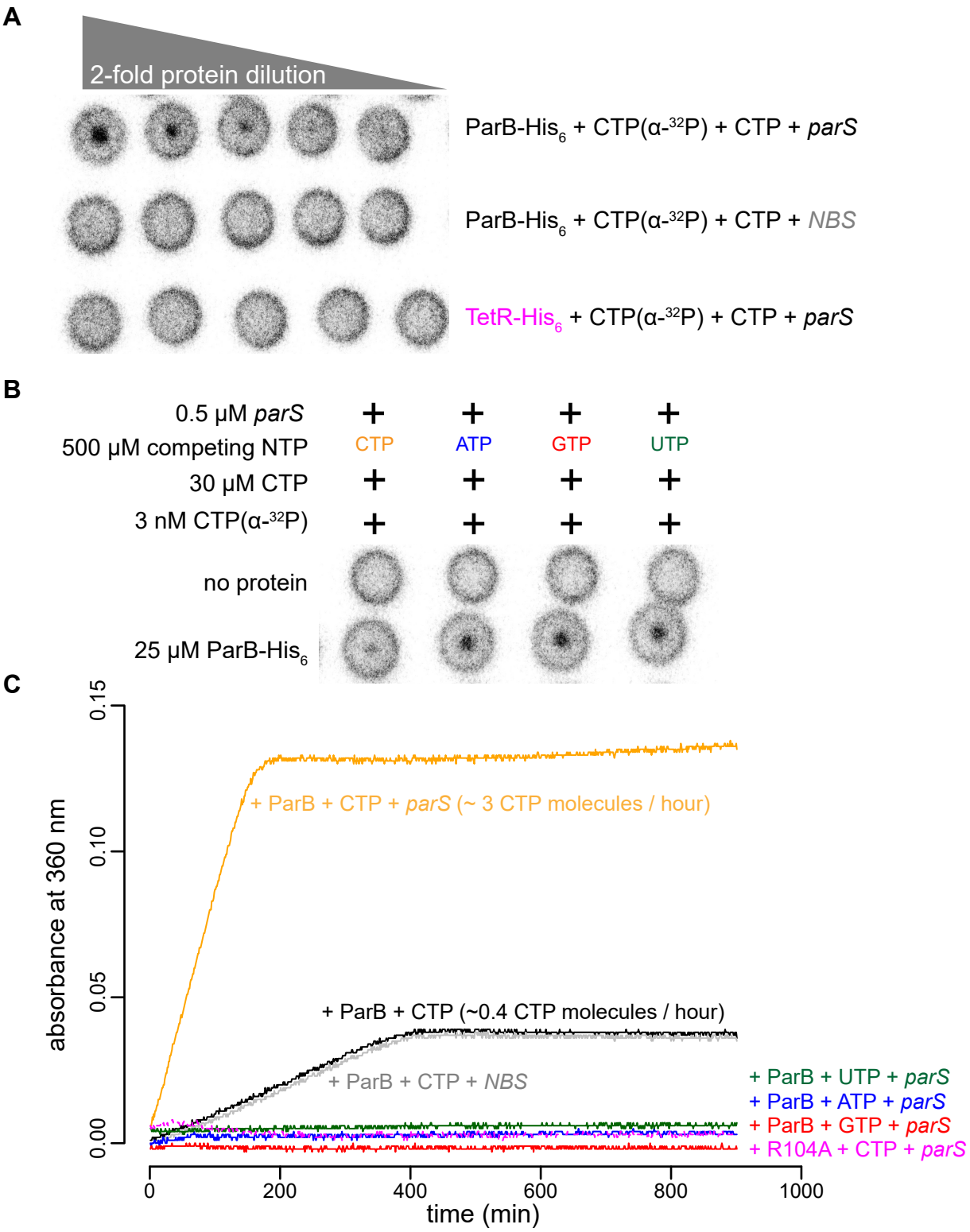

Figure 5. *parS* DNA increases the CTP binding and hydrolysis rate by *Caulobacter* ParB. (A-B) CTP binding as monitored by DRaCALA assay using radiolabeled CTP α-P^{32}. The bulls-eye staining indicates CTP binding due to a more rapid immobilization of protein-ligand complexes compared to free ligands alone. The starting concentration of proteins used in panel A was 25 μM. The same concentration of radioactive CTP, unlabeled CTP, and DNA was used in experiments shown in panels A and B. **(C)** A continuous monitoring of inorganic phosphate (Pi) released by recording absorbance at 360 nm over time at 25°C. The rates of CTP hydrolysis were inferred from a Pi standard. The NTP hydrolysis of *Caulobacter* ParB was also monitored in the presence of ATP, GTP, or UTP, with a 22-bp *parS* DNA duplex or a non-cognate 22-bp *NBS* DNA duplex (a DNA-binding site of Noc protein[48]). The nucleation-competent but spreading-defective ParB (R104A) mutant did not hydrolyze CTP in the presence of *parS* DNA.

FIG. 6

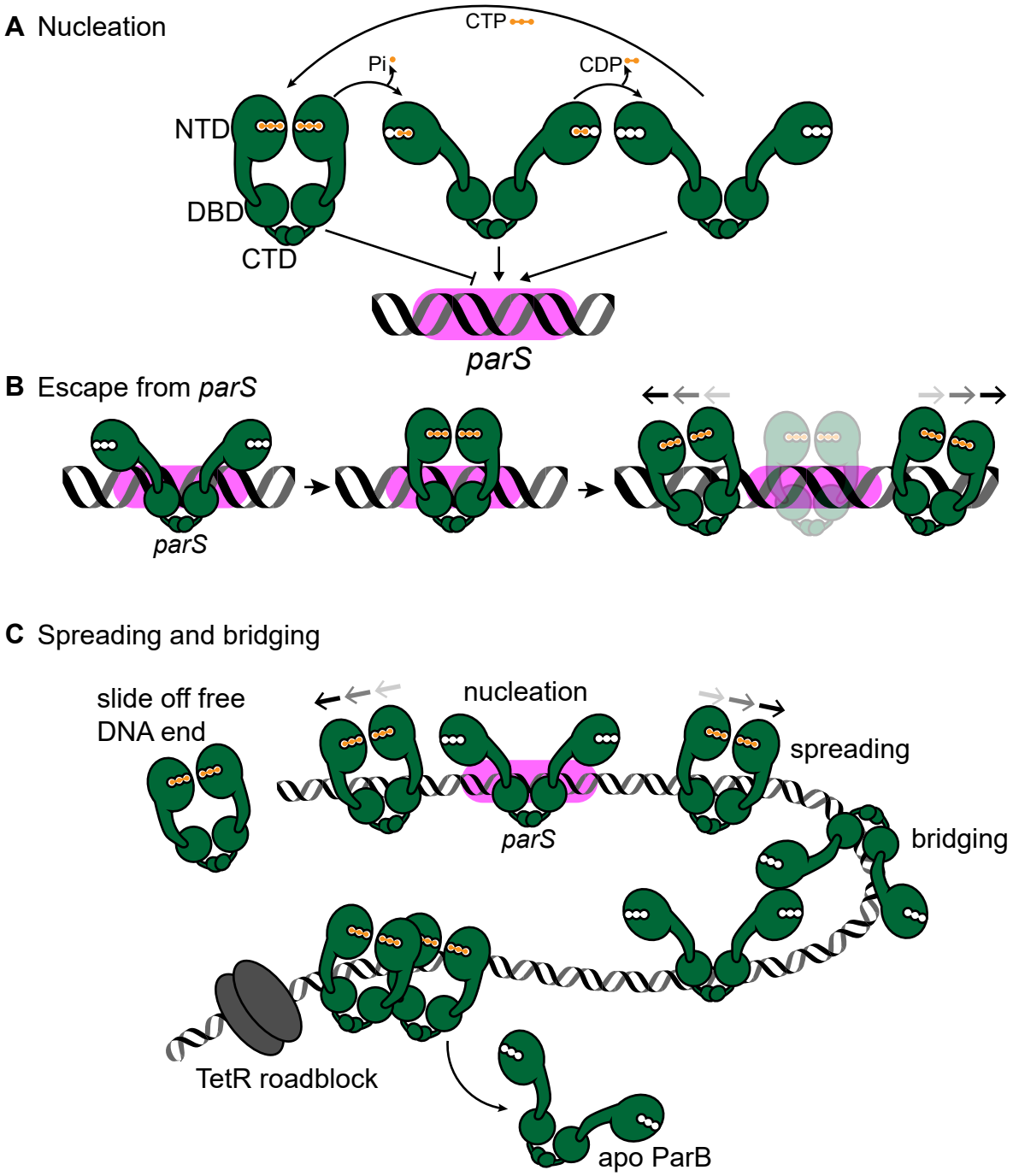

Figure 6. A model for *Caulobacter* ParB nucleation, spreading and bridging. (A) *Caulobacter* ParB nucleation at *parS*. CTP (orange) reduces *Caulobacter* ParB (dark green) nucleation at *parS* (magenta box), presumably by inducing conformational changes that are incompatible with a site-specific *parS* binding[44]. Only apo- or CDP-bound ParB can nucleate on *parS*. The domain architecture of ParB is also shown: NTD: N-terminal domain, DBD: DNA-binding domain, and CTD: C-terminal domain. **(B)** *Caulobacter* ParB escapes from the nucleation site *parS*. Apo-ParB at *parS* binds CTP and slides laterally away from the nucleation site *parS* while still associating with DNA. **(C)** *Caulobacter* ParB spreading and bridging on DNA *in vivo*. CTP-bound ParBs diffuse from the nucleation site *parS* and can run off the open DNA end unless they are blocked by DNA-bound roadblocks such as transcriptional regulators e.g. TetR. After CTP hydrolysis, ParB proteins that are already bound on DNA can bridge DNA together before dissociating to the solution. DNA-bridging and DNA-condensation activities have been observed for *Bacillus* ParB[19,20,40,41] but not for *Caulobacter* ParB[49] *in vitro*.

FIG. 1-figure supplement 1

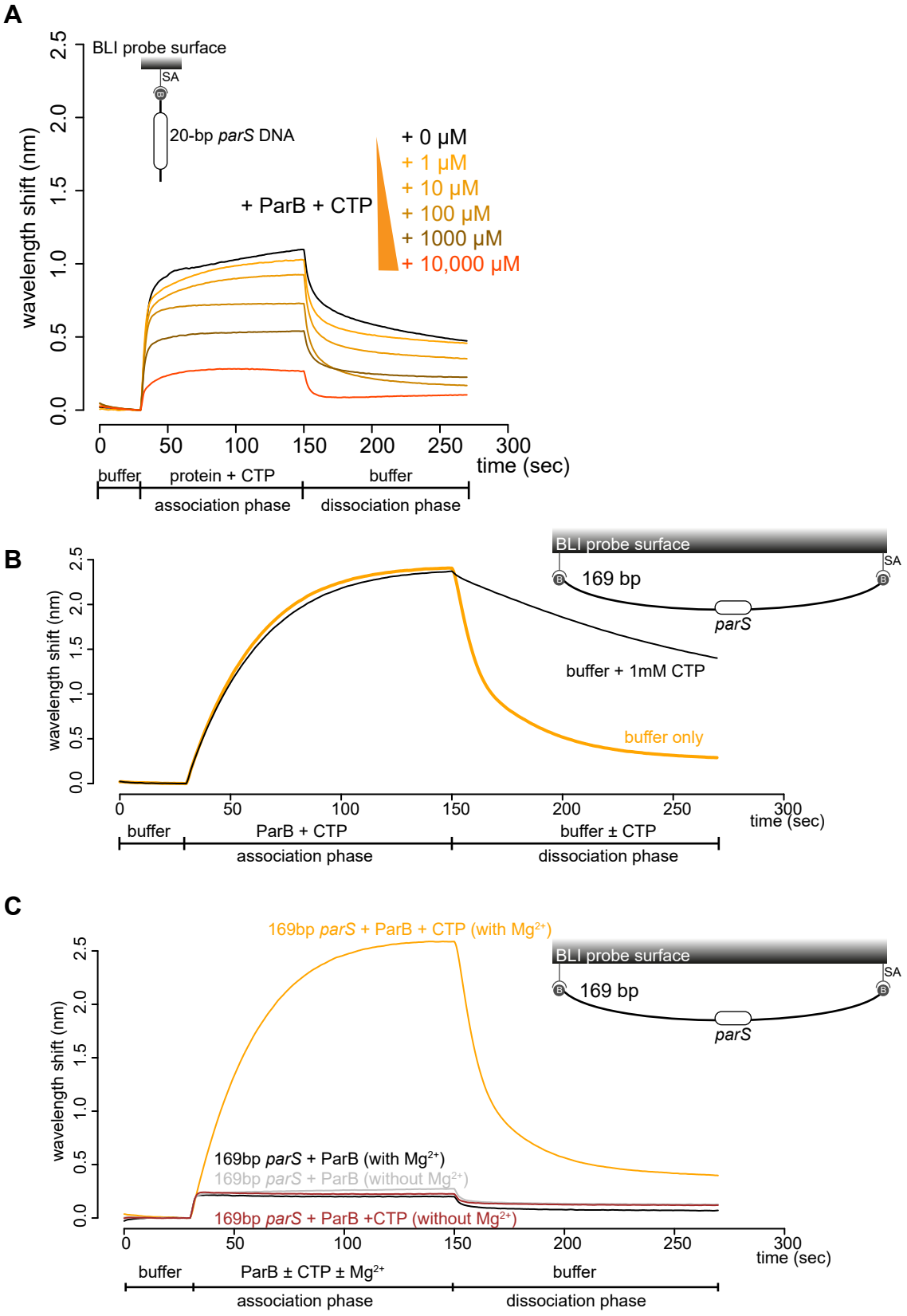

Figure 1-figure supplement 1. Cytidine triphosphate (CTP) modulates ParB nucleation and spreading on a *parS*-containing DNA substrate. (A) BLI analysis of the interaction between a premix of 1 µM His_6-tagged *Caulobacter* ParB and a 20-bp *parS* DNA probe in the presence of an increasing concentration of CTP. **(B)** BLI analysis of the interaction between 1 µM *Caulobacter* ParB-His_6 (with CTP) and a 169-bp dual biotin-labeled *parS* DNA. For the dissociation phase, the probe was returned to a buffer only or buffer supplemented with 1 mM CTP solution. **(C)** BLI analysis of the interaction between a premix of 1 µM *Caulobacter* ParB-His_6 ± 1 mM CTP and a 169-bp dual biotin-labeled DNA containing a *parS* or a scrambled *parS* site in buffer with or without $MgCl_2$. Schematics of the DNA substrate are shown above each sensorgram.

FIG. 2-figure supplement 1

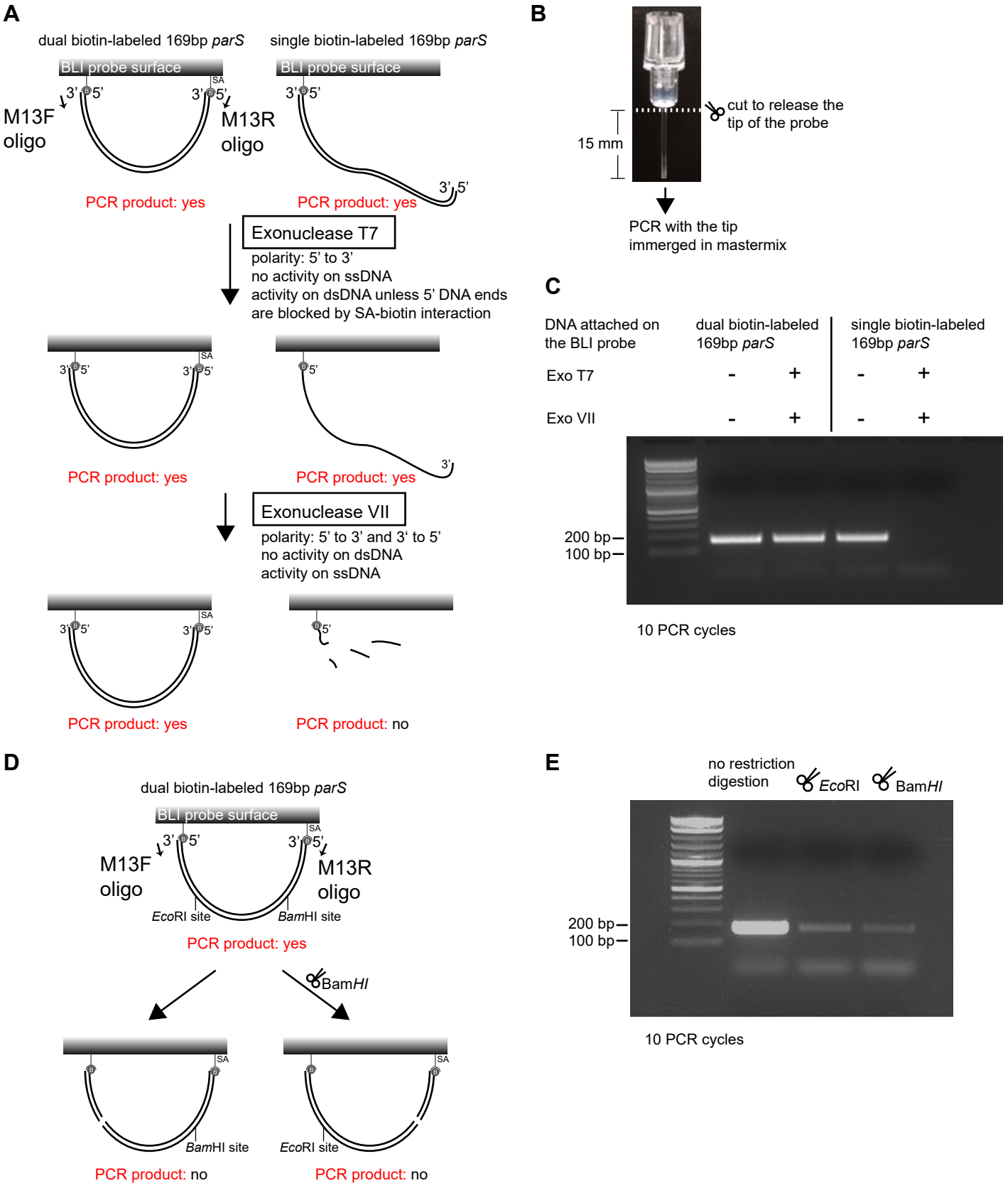

Figure 2-figure supplement 1. Dual biotin-labeled DNA fragments form a closed substrate on the surface of the BLI probe. (A) Schematic of the double digestion assay using Exonuclease T7 + Exonuclease VII and PCR. PCR was performed using M13F, M13R oligos, and DNA attached to the BLI surface as template. **(B)** The BLI probe was severed from the plastic adaptor and immerged into a PCR master-mix. **(C)** Dual biotin-labeled DNA fragments on the BLI surface were resistant to Exo T7 + Exo VII digestion while single biotin-labeled DNA fragments on the BLI surface was not. **(D-E)** Restriction enzymes cut and linearized DNA fragments on the BLI surface.

FIG. 2-figure supplement 2

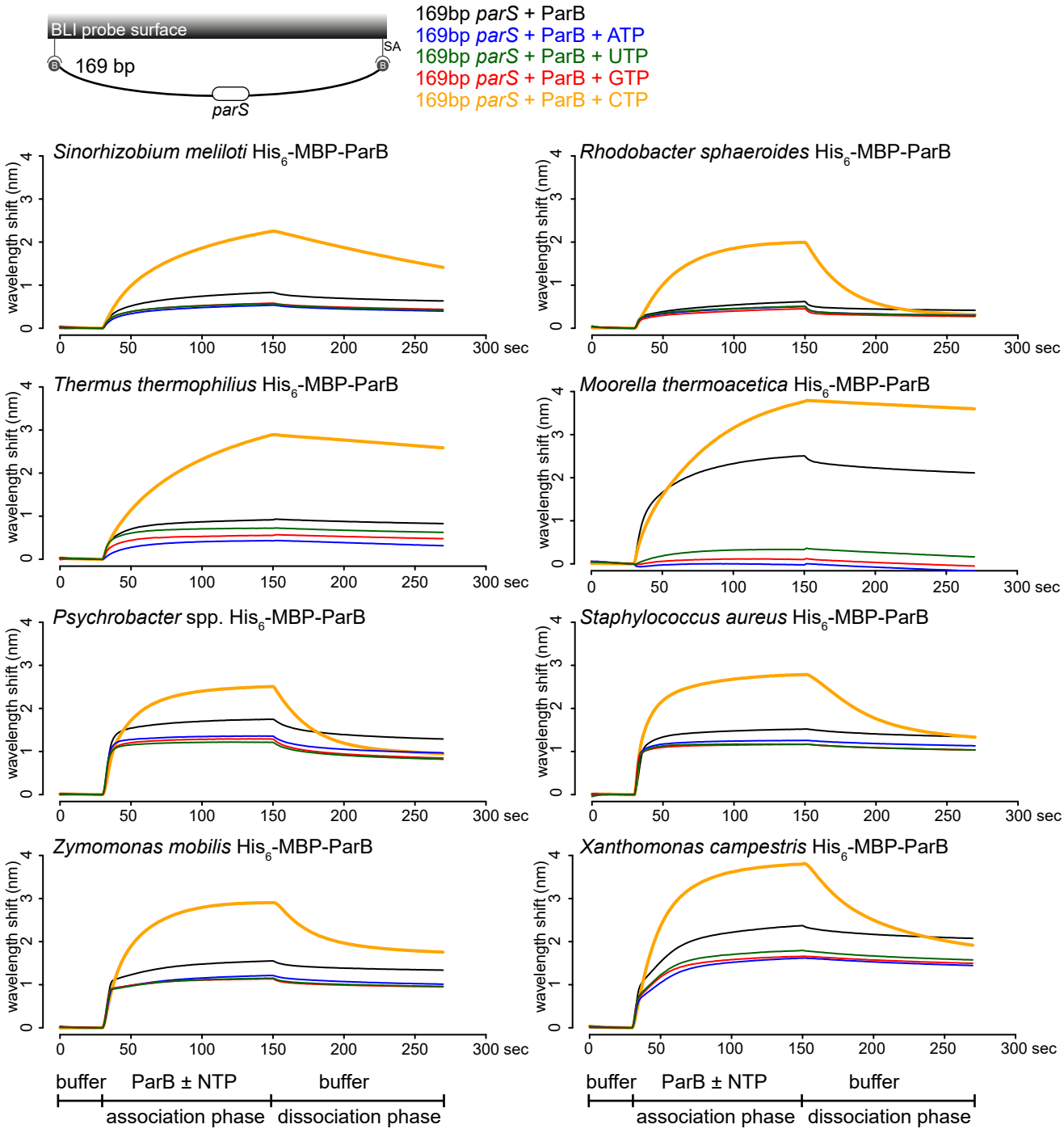

Figure 2-figure supplement 2. Cytidine triphosphate (CTP) facilitates ParB association with a closed DNA beyond nucleation. BLI analysis of the interaction between a premix of 1 μM His_6-MBP-tagged ParB from a set of diverse bacterial species ± 1mM NTP and a 169-bp dual biotin-labeled *parS* DNA. Schematics of the DNA substrate are shown above each sensorgram.

FIG. 2-figure supplement 3

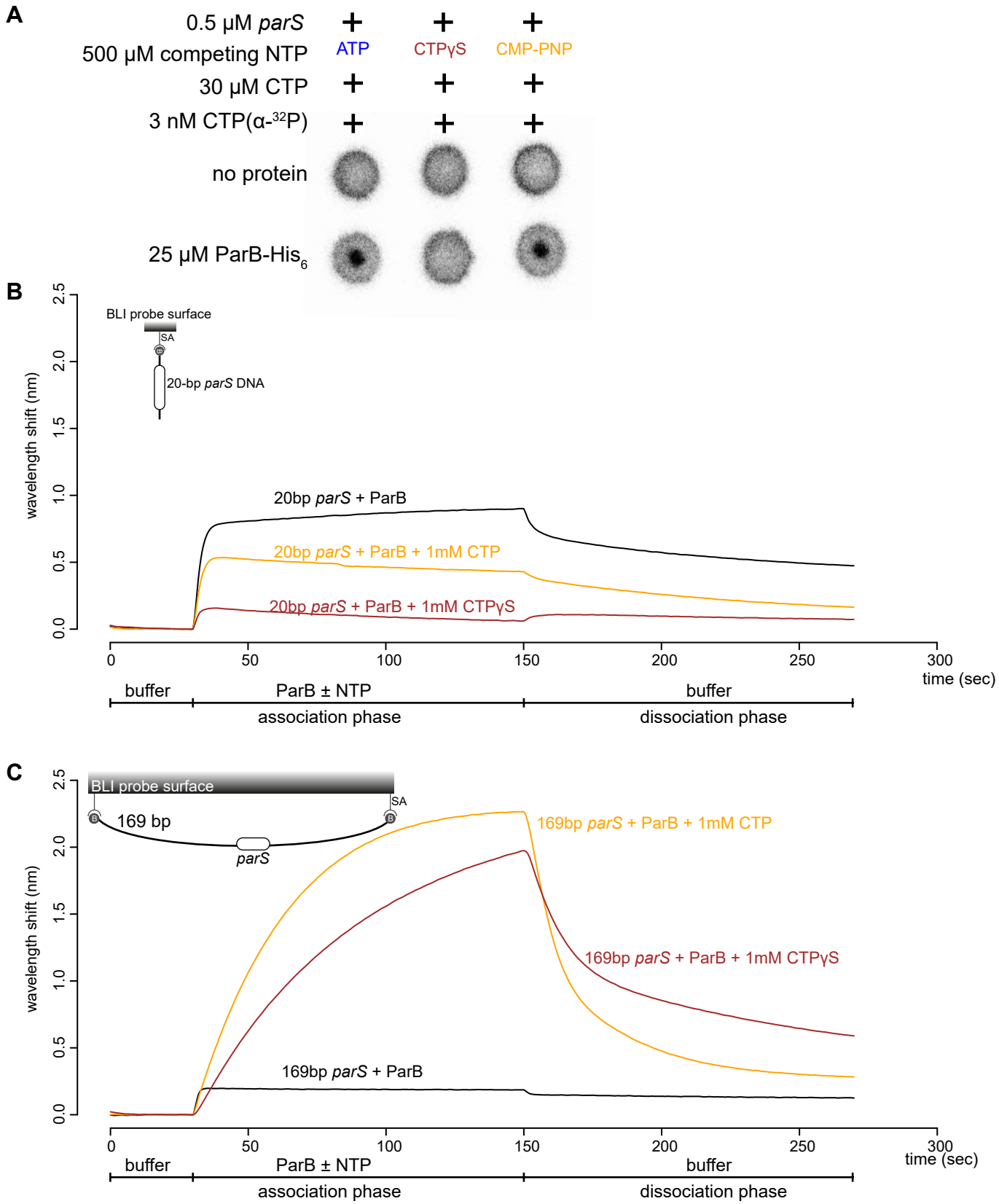

Figure 2-figure supplement 3. A non-hydrolysable CTP analog (CTPγS) modulates both the nucleation and spreading steps. (A) CTPγS (but not CMP-PNP) could outcompete radioactive CTP α-P32 for binding to ParB-*parS* complex, indicating that *Caulobacter* ParB can bind to CTPγS. Binding to radioactive CTP α-P32 was monitored by DRaCALA assay. The bulls-eye staining indicates CTP binding due to a more rapid immobilization of protein-ligand complexes compared to free ligands alone. **(B)** BLI analysis of the interaction between *Caulobacter* ParB-His_6 and a 20-bp *parS* DNA in the presence of CTP or CTPγS. **(C)** BLI analysis of the interaction between *Caulobacter* ParB-His_6 and a 169-bp *parS* DNA in the presence of CTP or CTPγS. Schematics of the DNA substrate are shown above each sensorgram.

SUPPLEMENTARY TABLE S1. PLASMIDS, DNA, AND PROTEIN SEQUENCES

Plasmids/DNA	Description	Source
pET21b::*Caulobacter* ParB-His_6	Overexpression of C-terminally His_6-tagged *Caulobacter* ParB, carbenicillin^R >*Caulobacter* ParB-His_6 MSEGRRGLGRGLSALLGEVDAAPAQAPGEQLGGSREAPIEILQRNPDQ PRRTFREEDLEDLSNSIREKGVLQPILVRPSPDTAGEYQIVAGERRWRA AQRAGLKTVPIMVRELDDLAVLEIGIIENVQRADLNVLEEALSYKVLMEKF ERTQENIAQTIGKSRSHVANTMRLLALPDEVQSYLVSGELTAGHARAIAA AADPVALAKQIIEGGLSVRETEALARKAPNLSAGKSKGGRPPRVKDTDT QALESDLSSVLGLDVSIDHRGSTGTLTITYATLEQLDDLCNRLTRGIKLAA ALEHHHHHH*	Gift from C. Jacob-Wagner[1]
pET21b::TetR-His_6	Overexpression of C-terminally His_6-tagged TetR (class B, from Tn10), carbenicillin^R >TetR (class B, from Tn10)-His_6 MSRLDKSKVINSALELLNEVGIEGLTTRKLAQKLGVEQPTLYWHVKNKRALL DALAIEMLDRHHTHFCPLEGESWQDFLRNNAKSFRCALLSHRDGAKVHL GTRPTEKQYETLENQLAFLCQQGFSLENALYALSAVGHFTLGCVLEDQEH QVAKEERETPTTDSMPPLLRQAIELFDHQGAEPAFLFGLELIICGLEKQLKC ESGSKLAAALEHHHHHH*	This study
pUC19::260bp-*parS*	pUC19 plasmid with 260-bp insert that contains *parS* sites, carbenicillin^R >260-bp_natural_*Caulobacter_parS*_fragment_cloned_into_pUC19 caagacgctcgcctcaatgcgaacgccccgggttcgagcgggggcg ctggactcgatctatacgccaatcaggcgagcgggtcgatgtgactcatc ggcgtttcacgtgaaacacccccaccgcagctgtgagcggcctgtggac aatattggggatgttccacgtgaaacatcacttgccgatacagaaggtcg aaaagacccgtccaagaacgtcctcaggatcgatacggccggagatg cgctccagggcccgggc	This study
pUC19::260bp-scrambled *parS*	pUC19 plasmid with 260-bp insert that contains scrambled *parS* sites, carbenicillin^R >260-bp_scrambled_*Caulobacter_parS*_fragment_cloned_into_pUC19	This study

	caagacgctcgcctcaatgcgaacgcccccgggttcgagcgggggcg ctggactcgatctatacgccaatcaggcgagcgggtcgatgtgactcatc ggacagctcgagattcatcccccaccgcagctgtgagcggcctgtggac aatattggggaatcgagtatacgctactcacttgccgatacagaaggtcg aaaagacccgtccaagaacgtcctcaggatcgatacggccggagatg cgctccagggcccgggc	
pET-His-MBP-TEV-DEST::*Sinorhizobium meliloti* ParB	For the purification of *Sinorhizobium meliloti* His_6-MBP-ParB	[2]
pET-His-MBP-TEV-DEST::*Rhodobacter sphaeroides* ParB	For the purification of *Rhodobacter sphaeroides* His_6-MBP-ParB	This study
pET-His-MBP-TEV-DEST::*Thermus thermophilus* ParB	For the purification of *Thermus thermophilus* His_6-MBP-ParB	[2]
pET-His-MBP-TEV-DEST::*Moorella thermoacetica* ParB	For the purification of *Moorella thermoacetica* His_6-MBP-ParB	This study
pET-His-MBP-TEV-DEST::*Psychrobacter* spp. ParB	For the purification of *Psychrobacter* spp. His_6-MBP-ParB	This study
pET-His-MBP-TEV-DEST::*Staphylococcus aureus* ParB	For the purification of *Staphylococcus aureus* His_6-MBP-ParB	[2]
pET-His-MBP-TEV-DEST::*Zymomonas mobilis* ParB	For the purification of *Zymomonas mobilis* His_6-MBP-ParB	This study
pET-His-MBP-TEV-DEST::*Xanthomonas campestris* ParB	For the purification of *Xanthomonas campestris* His_6-MBP-ParB	[2]
169bp_*parS*	cgccagggttttcccagtcacgacgttgtaaaacgacggccagtgaattcgagctcggtac ccgcaggaggacgtagggtaggggga**tgtttcacgtgaaaca**ggggatcctctagagtc gacctgcaggcatgcaagcttggcgtaatcatggtcatagctgtttcct	This study
169bp_scrambled_*parS*	cgccagggttttcccagtcacgacgttgtaaaacgacggccagtgaattcgagctcggtacc cgcaggaggacgtagggtaggggga***aattacactgagttta***ggggatcctctagagtcga cctgcaggcatgcaagcttggcgtaatcatggtcatagctgtttcct	This study
170bp_*parS*	cgccagggttttcccagtcacgacgttgtaaaacgacggccagaattcgcaacgtg **tgtttcacgtgaaaca**gccttgaactgataacgactctatcattgatagagtgttctct ccacgggatccccaggcatgcaagcttggcgtaatcatggtcatagctgtttcct	This study
around_pUC19_F	tcactcatggttatggcagcactgcataattc	This study

around_pUC19_F	taacactgcggccaacttacttctgacaacg	This study
20bp_*parS*_BLI_probeF	[Biotin]GGGAtgTTTCACGTGAAAca	This study
20bp_*parS*_BLI_probeR	tgTTTCACGTGAAAcaTCCC	This study
28bp_*tetO*_BLI_probeF	[Biotin]ggggactctatcattgatagagtatgc	This study
28bp_*tetO*_BLI_probeR	gcatactctatcaatgatagagtcccc	This study
20bp_*NBS*_BLI_probeF	[Biotin]GGGAtaTTTCCCGGGAAAta	This study
20bp_*NBS*_BLI_probeR	taTTTCCCGGGAAAtaTCCC	This study

Keys:
M13F (-47): cgccagggttttcccagtcacgac M13R: aggaaacagctatgaccat
parS: **tgtttcacgtgaaaca** scrambled *parS*: ***aattacactgagttta***
tetO: actctatcattgatagagt BamHI RS: ggatcc EcoRI RS: gaattc HindIII RS: aagctt

SUPPLEMENTARY REFERENCES

1. Lim, H. C. *et al.* Evidence for a DNA-relay mechanism in ParABS-mediated chromosome segregation. *Elife* **3**, e02758 (2014).

2. Jalal, A. S. B. *et al.* Evolving a new protein-DNA interface via sequential introduction of permissive and specificity-switching mutations. *bioRxiv* 724823 (2019) doi:10.1101/724823.